

# a new membrane-aerated biofilm reactor for low energy wastewater treatment: pilot results

Presented at WEFTEC Conference, 2015.

## Authors:

Pierre Côté<sup>1</sup>, Jeff Peeters<sup>2</sup>, Nicholas Adams<sup>2</sup>, Youngseck Hong<sup>2</sup>, Zebo Long<sup>2</sup>, John Ireland<sup>2</sup>

<sup>1</sup> COTE Membrane Separation Ltd, Hamilton, Ontario

<sup>2</sup> SUEZ Water Technologies & Solutions, Oakville, Ontario

## abstract

A new hybrid membrane-aerated biofilm reactor (MABR) technology that enables energy-neutral treatment of municipal wastewater is introduced. The process, which removes nitrogen using conventional nitrification-denitrification, was demonstrated at pilot-scale, treating primary effluent. The new MABR membrane product can operate in a high mixed liquor suspended solids (MLSS) environment, making it suitable for use in a conventional activated sludge reactor to increase oxygen transfer and nitrification capacity. The pilot achieved removal rates of 91% for TSS, 83% for COD, 95% for ammonia, and 66% for total inorganic nitrogen. MABR technology has the potential to transfer oxygen very efficiently, at an aeration efficiency of 6 kg O<sub>2</sub>/kWh.

**Keywords:** Membrane-aerated biofilm reactor, integrated fixed-film activated sludge, energy-neutral wastewater treatment.

## introduction

A biological process that enables energy-neutral treatment of municipal wastewater was introduced by Peeters et al (2014a). The process is a hybrid membrane-aerated biofilm reactor (MABR) that removes nitrogen using the conventional nitrification-denitrification pathway.

An MABR offers all the benefits of biofilm reactors with, in addition, the ability to transfer oxygen very efficiently and at low energy input. Oxygen is transferred without bubbles through a gas-transfer membrane, which favors the establishment of a nitrifying biofilm. In a hybrid MABR process, the membranes are immersed in a suspended biomass that is kept anoxic or micro-aerobic for denitrification.

The new MABR product and its performance treating a synthetic ammonia solution were described by Adams et al (2014). This paper presents the results of a 220 day study treating primary effluent using pilot-scale modules.

Find a contact near you by visiting [www.suezwatertechnologies.com](http://www.suezwatertechnologies.com) and clicking on "Contact Us."

\*Trademark of SUEZ; may be registered in one or more countries.

©2017 SUEZ. All rights reserved.

## new membrane-aerated biofilm reactor technology

The building block of the new MABR membrane is an unbreakable “cord”, which is constructed of dense-wall, oxygen-permeable hollow fiber membranes distributed around the circumference of a yarn reinforcement core (Figure 1). A cord has a diameter of about 1.1 mm and is designed to be deployed in a module approximately 2 m long.

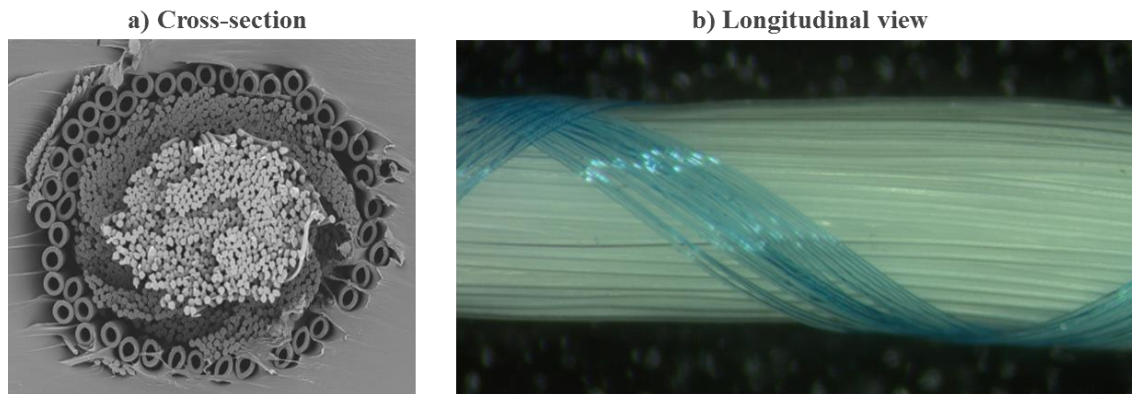


**Figure 1. Cord structure**

The new MABR module has two thin/elongated headers for air feed and exhaust and contains thousands of cords. The cords are geometrically spaced apart in the headers and mounted with slack to allow free swaying. Modules are assembled into cassettes (Figure 2). An air scouring system at the bottom of the cassette has been adapted to mix wastewater inside the cord bundles and control biofilm thickness.



**Figure 2. New MABR cassette**

Oxygen transfer performance with an MABR is a function of the membrane characteristics and operational parameters that are similar to fine bubble aeration systems. Because the biofilm surface area changes with the biofilm thickness (and the biofilm thickness is not normally known), performance is expressed on the basis of “surface area of cord”, using a cord outside diameter of 1.1 mm.

In an MABR, it is easy to perform an oxygen mass balance on the gas side because the exhaust gas is contained and key variables (flow and oxygen concentration) can be measured on a continuous basis (this would be analogous to measuring oxygen transfer efficiency with the off-gas method on a continuous basis in a bubble aeration system). The primary parameter determined from experimental data is the oxygen flux through the membranes:

$$J = \frac{24 \cdot M_O}{V_m} (Q_{PF} \cdot X_F - Q_{PE} \cdot X_E) \quad \text{Equation 1}$$

where:  $J$  = oxygen flux (g O<sub>2</sub>/d/m<sup>2</sup>)

$M_O$  = oxygen molecular weight (32 g/mol)

$Q_{PF}$ ,  $Q_{PE}$  = process gas feed and exhaust specific flow rates (Nm<sup>3</sup>/h/m<sup>2</sup>)

$V_m$  = standard gas volume at STP (0.0224 m<sup>3</sup>/mol)

$X_F$ ,  $X_E$  = molar fraction of oxygen in feed and exhaust gas (-)

The oxygen transfer rate (OTR) is directly proportional to the surface area of membrane deployed:

$$OTR = J \cdot S \quad \text{Equation 2}$$

where  $OTR$  = oxygen transfer rate (g O<sub>2</sub>/d)

$S$  = surface area of cord (m<sup>2</sup>)

There is a simple relationship between the oxygen flux and the oxygen transfer efficiency (OTE):

$$OTE = \frac{J}{24 \cdot Q_{PF} \cdot M_O \cdot X_F} \quad \text{Equation 3}$$

where all the terms have been previously defined.

When designing an activated sludge aeration system, the power input for the blower is calculated two different ways – first to meet the oxygen demand and second to keep the mixed liquor in suspension – and the higher of the two values determines the blower size. A similar situation exists for an MABR: there is a power input component required for aeration to meet the oxygen demand and a second component to provide mixing on the liquid side to promote substrate penetration into the biofilm (i.e.; renew the boundary layer). Mathematically, the aeration efficiency can be expressed as follows:

$$\frac{1}{AE} = \frac{24}{J \cdot V_m} (W_P \cdot Q_{PF} + f \cdot W_M \cdot Q_M) \quad \text{Equation 4}$$

where: AE = aeration efficiency (kg O<sub>2</sub>/kWh)

*f* = mixing time fraction (-)

Q<sub>M</sub> = specific mixing gas flow rate at STP (Nm<sup>3</sup>/h/m<sup>2</sup>)

W<sub>P</sub>, W<sub>M</sub> = adiabatic compression energy for the process  
and mixing gas blowers (Wh/mol air)

In Equation 4, the two terms on the right side have units of kWh/kg O<sub>2</sub> and represent the specific energy to cause the reactants to meet in the biofilm: the first term for oxygen and the second term for the substrate.

The adiabatic compression energy *W* in Equation 4 is calculated with:

$$W = 3,600 \frac{1}{e} \frac{RT}{(k-1)/k} \left[ \left( \frac{P_2}{P_1} \right)^{(k-1)/k} - 1 \right] \quad \text{Equation 5}$$

where: *e* = blower / motor efficiency factor (0.65)

*k* = ratio of specific heat of air at constant pressure / constant volume = 1.395

P<sub>2</sub>/P<sub>1</sub> = absolute pressure after/before compression

R = gas law constant (8.314 J/°K)

T = absolute temperature (293.1 °K)

Conversion factor = 3,600 J/Wh

## materials and methods

Pilot-scale modules were built with small square headers and 1.8 m of exposed cord length. Each module contained 600 cords, for an approximate surface area of 3.5 m<sup>2</sup> per module. Each cord contained 48 hollow fibers distributed around the circumference of the yarn reinforced core as shown in Figure 1.

The pilot was located at Environment Canada's Wastewater Technology Centre (Burlington, Ontario, Canada) where raw wastewater from the nearby Skyway wastewater treatment plant is available via pipeline. The raw wastewater was treated with a rotating belt sieve that removed on average 66% TSS and 30% COD (Peeters et al, 2014b). The biological reactor consisted of three 100L tanks in-series, each containing one membrane module (Figure 3).

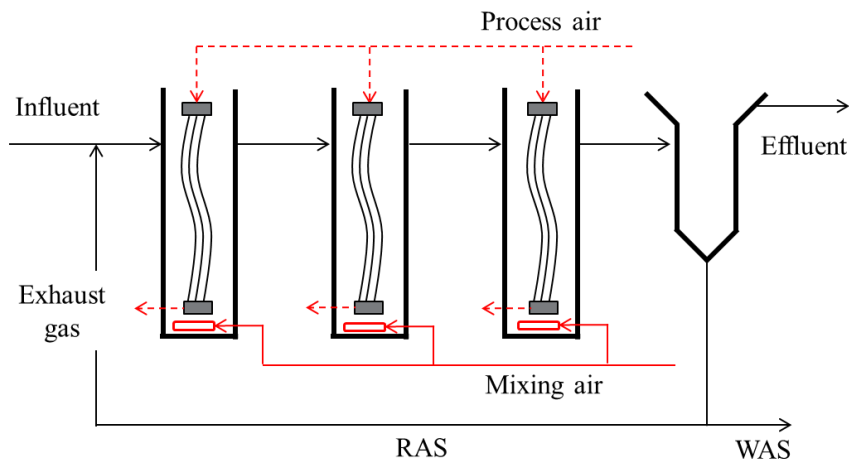


**Figure 3. Hybrid MABR pilot configuration**

Given the scale of the pilot, air from a compressor was used for process feed and tank mixing; however, energy calculations were made with equations 4 and 5 assuming that, at a larger scale, a blower would be used.

Process air was supplied at a pressure of 67 kPa and a constant flow rate,  $Q_{PF}$ , of 5.3 L/h/m<sup>2</sup> (at standard temperature and pressure). The exhaust gas flow rate was discharged at a pressure of 25 kPa; the exhaust gas flow rate was only measured sporadically and was equal to about 85% of the feed flow rate (i.e.; 4.5 L/h/m<sup>2</sup> (at standard temperature and pressure)). The oxygen concentration in the exhaust gas from each of the three modules was monitored on a continuous basis. The experimental oxygen flux was calculated from a mass balance on the process gas using Equation 1.

The tanks were mixed by coarse bubble sparging at a pressure of 25 kPa to overcome the static head above the sparging device. Mixing was intermittent with a cycle of 12s on / 108s off (i.e.;  $f$  equal to 0.1 in Equation 4) at a specific mixing gas flow rate,  $Q_m$ , of 28 L/h/m<sup>2</sup> (at standard temperature and pressure); this represented conditions at full-scale where a blower would run continuously and valves would direct the air to 10 different membrane units on a rotation basis. Sparging contributed negligible oxygen transfer.

The 300 L secondary clarifier was operated at a hydraulic loading rate of 0.2 m/h. Other than the return activated sludge (RAS) flow, there was no nitrate recycle in the process.

Key operating conditions for the 220 day pilot study are described in Table 1, divided into 3 periods. Period I (0-40d) corresponded to full development of the biofilm. Period II (41-120d) is the most representative from a process point of view. During Period III (121-220d), the influent characteristics were variable because the feed pipeline was shut-down for repair and wastewater was trucked in.

**Table 1. Pilot overview**

Period	I	II	III
Time (days)	0 – 40	41 – 120	121 – 220
Feed source	Pipeline plus primary treatment		Trucked wastewater plus primary treatment
Nitrification	Primarily by the suspended biomass	Primarily in the biofilm	
Denitrification	No denitrification high DO	Good denitrification rbCOD available	Poor denitrification little rbCOD available
Mixed liquor suspended solids	Ranged 1500-2500 mg/L, from biofilm sloughing and suspended growth		Peaked due to initial high SS of primary effluent
Results significance	Start-up biofilm growth	Representative hybrid operation	Non-representative Ohybrid operation

## results

The primary effluent feed was a typical dilute wastewater with a small soluble organic fraction of about 13% and a COD/BOD ratio of 1.84 (Table 2).

The pilot was fed at a constant feed flow rate of 40 L/h (hydraulic retention time of 7.5 h) and the return activated sludge flow rate was set to 40 or 60 L/h (Figure 4a). Solids retention time (SRT) was controlled at 7.5 d and resulted in mixed liquor suspended solids (MLSS) concentration varying between 1,500 and 2,500 mg/L (Figure 4b), except when wastewater trucking started (day 120 to 135) when it reached 5,000 mg/L. This was due to higher than normal values of TSS in the trucked wastewater.

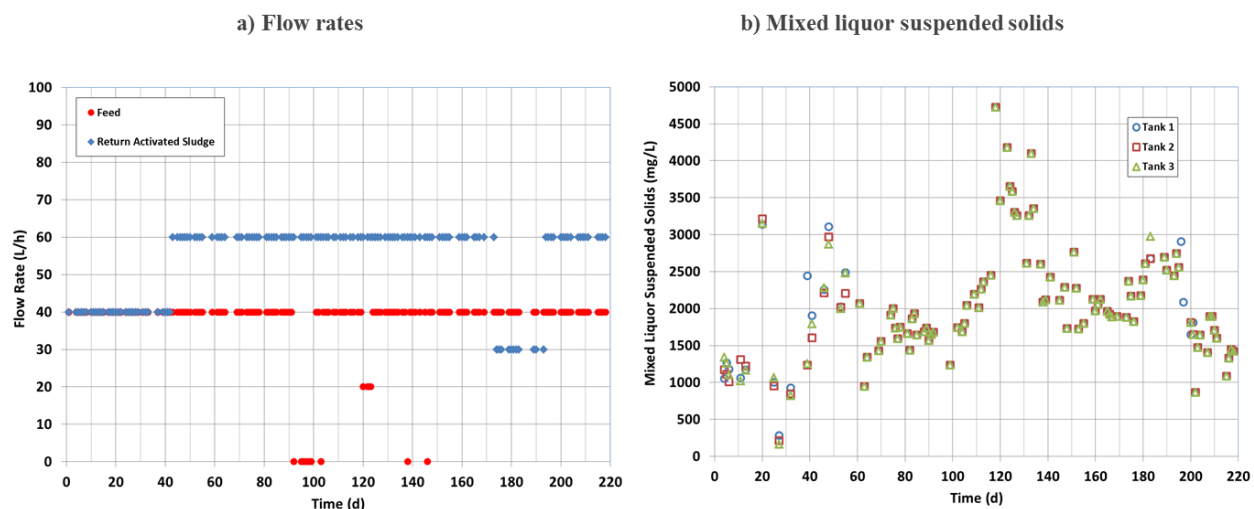


**Figure 4. Flow rates and mixed liquor suspended solids**

Dissolved oxygen reached saturation during period I when the membranes initially transferred oxygen into the bulk, but eventually decreased to less than 1 mg/L as the biofilm grew. The anoxic/micro-aerobic conditions in the bulk did not affect the sludge volume index which remained <100 mL/g (except for some deterioration during the trucking Period III).

**Table 2. Influent characteristics for all three periods (primary effluent)**

Parameter	Data Points	Median (mg/L)	Range (mg/L) 5%-95% percentile
TSS	122	144	44 – 270
COD	123	239	98 – 440
Soluble COD (0.45 $\mu$ m)	29	32	20 – 65
BOD	11	174	58 – 342
NH <sub>4</sub> -N	128	23.7	10.6 – 33.4

Treatment results are presented in Figure 5. Median removals for all three periods were: TSS 91%, COD 83%, NH<sub>4</sub> 95% and TIN 47%. For Period II only (considered more representative), performance was similar for all parameters except TIN, which increased to 66% due to a higher concentration of readily biodegradable COD (or BOD) for denitrification.

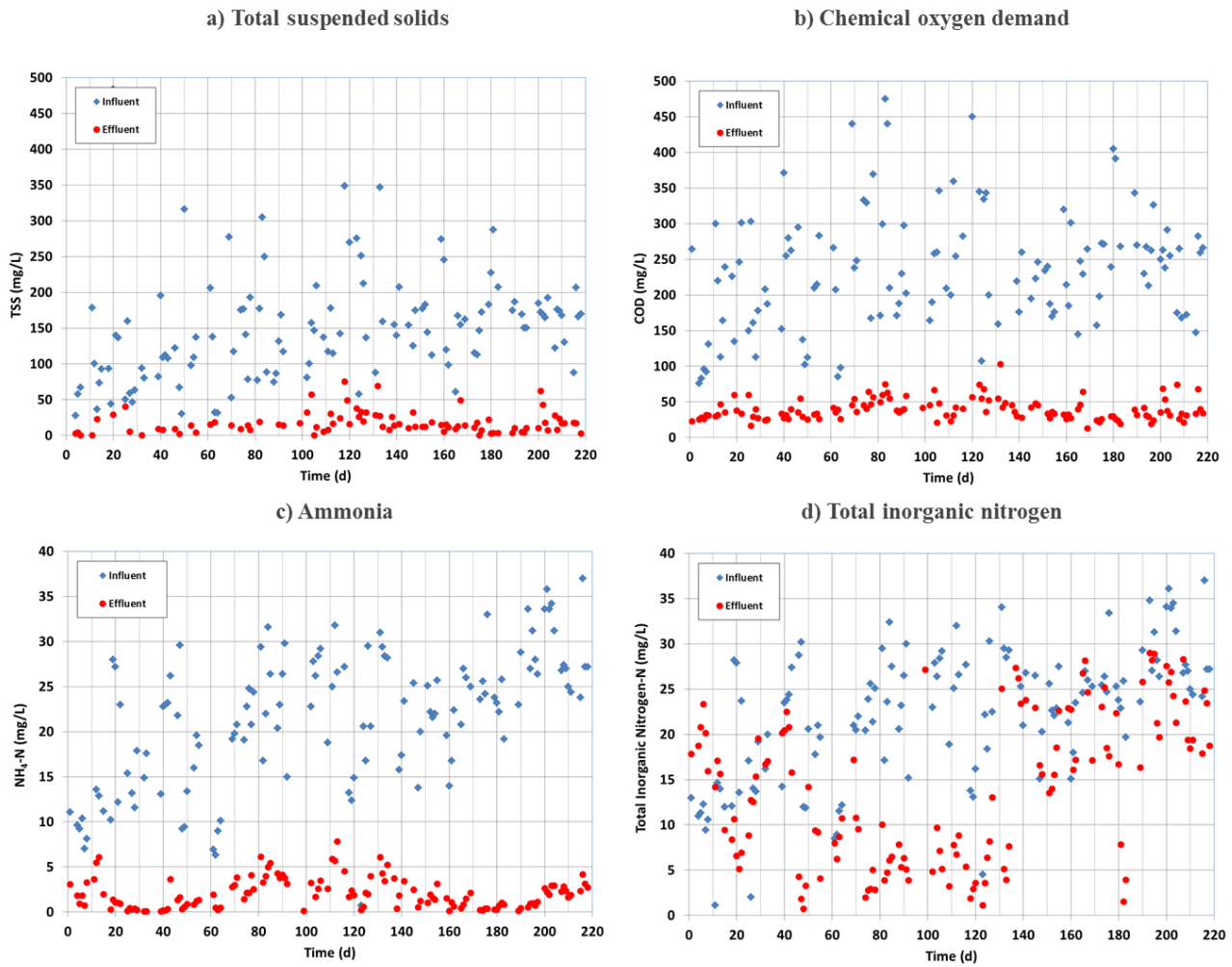


**Figure 5. Treatment results**

The oxygen flux ( $J$ , Equation 1) along with the oxygen transfer efficiency (OTE, Equations 3) are plotted in Figure 6a. These two parameters represent the same data, which is why the curves are identical, but off-set. The concentration of oxygen in the exhaust gas,  $X_e$ , ranged between 12 and 16%. The oxygen flux gradually increased from 8 to about 15 g/d/m<sup>2</sup> from the start of the study to day 90. OTE ranged between 30 and 40%. After the biofilm was established, the aeration efficiency (AE, calculated with Equation 4) which includes both the energy to pressurize the process air and sparging air sources ranged between 3 and 4 kg O<sub>2</sub>/kWh (Figure 6b).

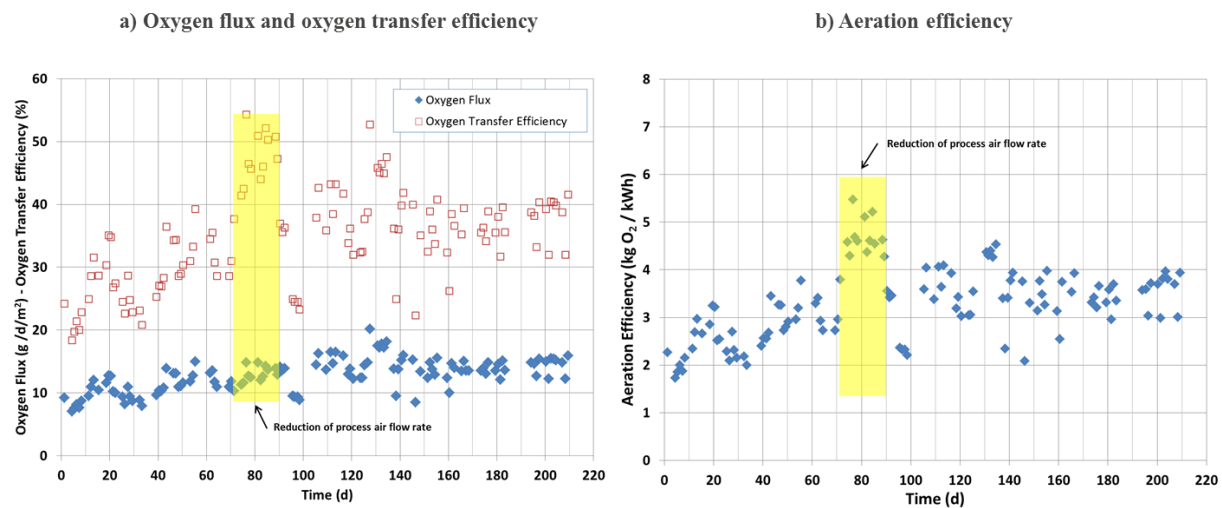


**Figure 6. Oxygen transfer**

Over a period of 20 days [71-90], the membrane process air feed conditions were changed to observe the impact on performance; the process air flow was reduced by 29% (from 5.3 to 3.8  $\text{L/h}/\text{m}^2$  (at standard temperature and pressure)) which resulted in reducing the feed pressure by 19% (from 67 to 54 kPa), without changing the exhaust discharge pressure of 25 kPa. During that period, OTE increased above 50% (Figure 6a, shaded area) without a negative impact on oxygen flux, an indication that the initial process air flow rate might have been too high and that an active biofilm draws out the oxygen that it needs; under these conditions, AE increased above 5  $\text{kg O}_2/\text{kWh}$  (Figure 6b, shaded area).

The nitrification rate for all 3 tanks together is plotted in Figure 7. Through Period II, the nitrification rate ranged between 1.5 and 2.5  $\text{g NH}_4\text{-N}/\text{d}/\text{m}^2$ . It reached 3  $\text{g NH}_4\text{-N}/\text{d}/\text{m}^2$  in Period III when the ammonia concentration increased (Figure 5c).

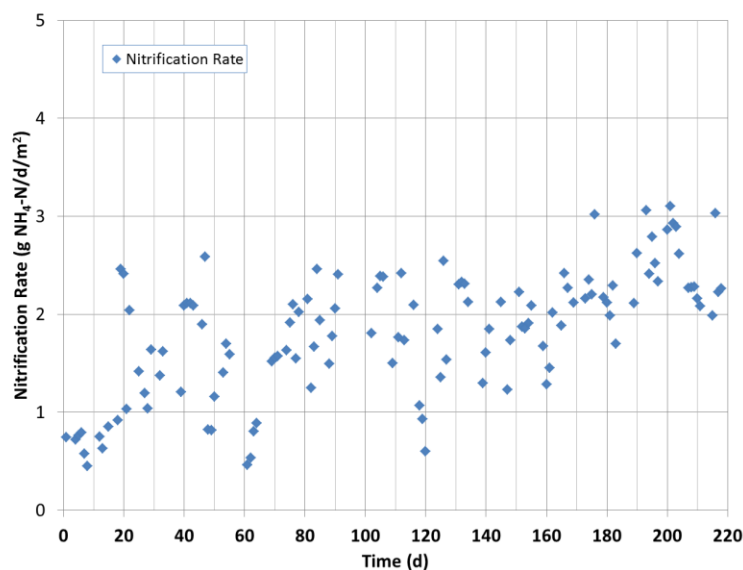


**Figure 7. Nitrification Rate**



Nitrification rates are compared to ammonia loading rates for all three tanks together in Figure 8a. The data points are close to the 45 degree line, an indication that the available biofilm surface area was not overloaded; for any data point, the ratio of nitrification rate over ammonia loading rate is equal to the ammonia removal rate (i.e.; >90%). The same information is plotted for individual tanks in Figure 8b. The scale is broader, with loading rates for Tank 1 reaching 12 g  $\text{NH}_4\text{-N/d/m}^2$  and nitrification rates reaching 6 to 8 g  $\text{NH}_4\text{-N/d/m}^2$ . At low loading rates (i.e.; in Tank 3), the nitrification rates fell on or close to the 45 degree line, indicating quasi total removal; as the loading rate increased, the data are more variable and the nitrification rate was equal to about one-half of the loading rate (i.e.; about one-half of the ammonia was nitrified in Tank 1).

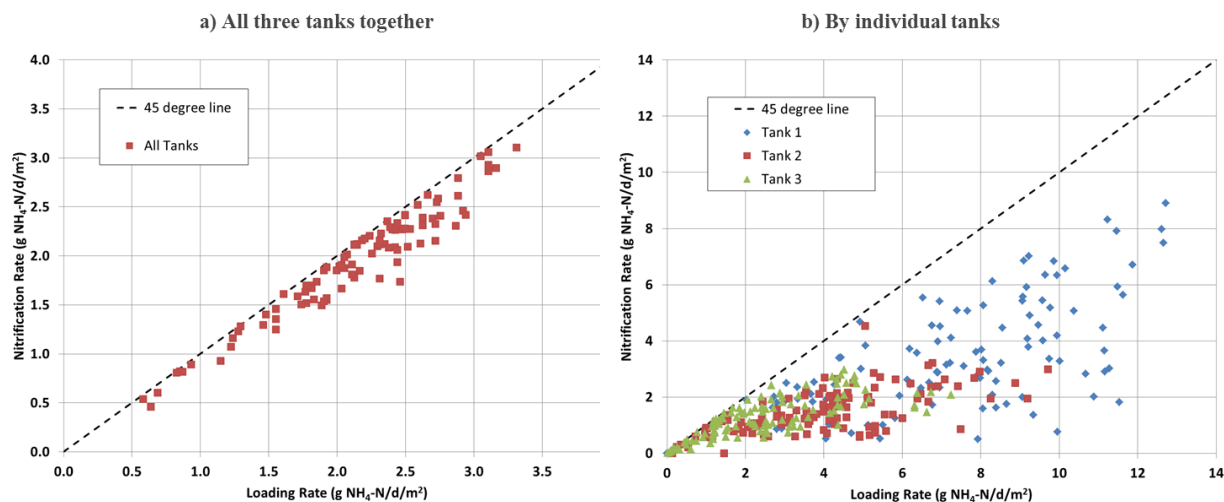


**Figure 8. Ammonia loading and nitrification rates**

## discussion

### nitrification rate compared to conventional biofilm processes

Conventional and membrane-supported biofilms are compared schematically in Figure 9. Figure 9a shows that with a conventional biofilm the reactants (oxygen and substrate) approach the biofilm from the bulk liquid and that the bio-chemical conversion is a "surface reaction". However, with a membrane-supported biofilm (Figure 9b) oxygen and substrate approach the biofilm from opposite sides and must meet by diffusion for the reaction to take place "within the biofilm". This fundamental difference favors the establishment of a nitrifying biofilm even in the presence of significant readily biodegradable COD (rbCOD) and competition from heterotroph bacteria. The reason is that ammonia is a small molecule that diffuses much faster than organic molecules within the biofilm. According to Stewart (2003), the ratio of the effective diffusion coefficients of ammonia over acetate or sucrose (small organic molecules representative of rbCOD) in biofilms is about 10. Therefore, because the biofilm is normally thick enough to prevent oxygen from reaching the bulk liquid, substrate molecules must diffuse into the biofilm for the conversion to take place, and this favors autotrophic reactions versus heterotrophic reactions.

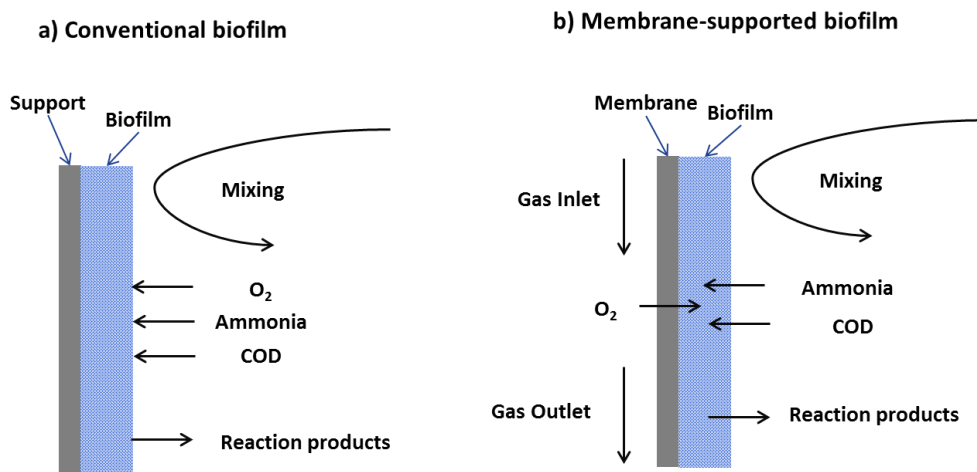


**Figure 9. Conventional and membrane-supported biofilms**

To illustrate this point, the data from Figure 8b are plotted in Figure 10 as red squares. They represent performance for a C/N ratio of 7.3 in this study (BOD/ $NH_4$ -N in Table 2). A similar set of results from a different study obtained with a synthetic ammonia solution having a C/N ratio of 0.5 are plotted as blue triangles (Adams et al, 2014). The presence of organic carbon in this study did not cause a significant decrease in nitrification rates. This observation contrasts sharply with conventional nitrifying biofilm processes which are very sensitive to C/N ratio due to competition between nitrifying autotrophs and carbon oxidizing heterotrophs (WEF, 2011).

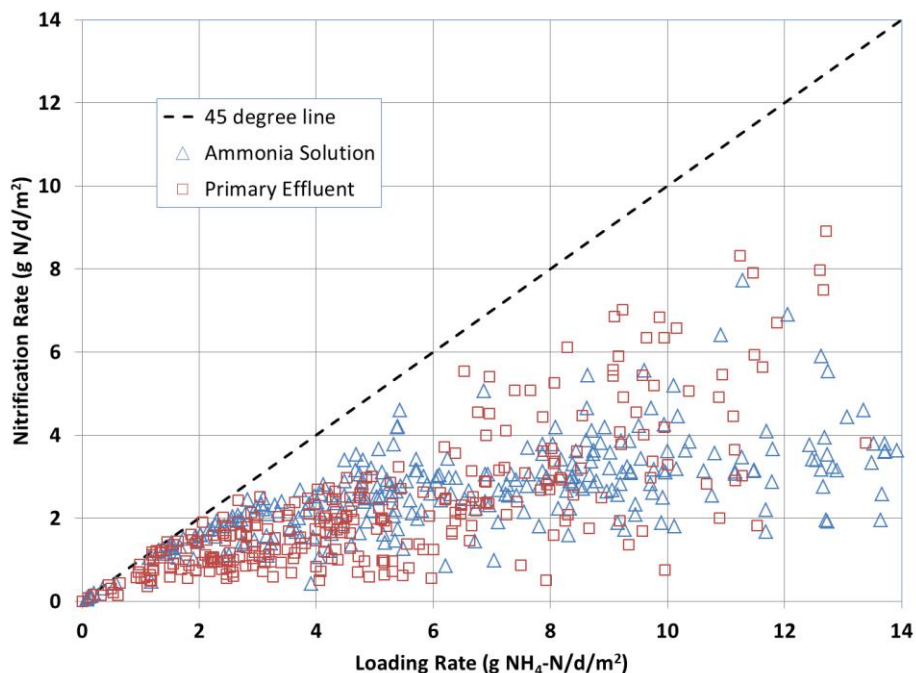


**Figure 10. Impact of C/N ratio on nitrification rate**

The nitrification rates measured in this study of 1 to 3 g  $\text{NH}_4\text{-N/d/m}^2$  compare advantageously to other MABR results (Syron and Casey, 2008; Martin and Nerenberg, 2012) and to tertiary nitrification on inert media, either fixed or moving bed (WEF, 2011).

A rough oxygen mass balance during Period II provides insight into how the process works. The average OTR was 150 g  $\text{O}_2/\text{d}$  (15 g  $\text{O}_2/\text{d/m}^2 \times 10 \text{ m}^2$  cord) and the average nitrification rate was 22 g N/d. Using the stoichiometric value of 4.57 g  $\text{O}_2/\text{g N}$ , the amount of oxygen required for nitrification was equal to 100 g  $\text{O}_2/\text{d}$ , or about 67% of the oxygen transfer rate. During that period, the total inorganic nitrogen was reduced by 15 g/d (22 to 7.5 mg/L or 66% removal in Figure 5d). Assuming an organic carbon requirement of 5 g COD/g N for denitrification, the amount of COD needed for denitrification was 75 g/d (78 mg/L). Comparing this requirement to the reduction of sCOD (data not shown), it can be concluded that denitrification was limited by the availability of readily biodegradable COD.

### **mixing energy**

In Equation 4, the second term ( $W_m \cdot f \cdot Q_m / V_m$ ) is a specific mixing power input,  $P_m$ . The level of  $P_m$  used in the study (0.03  $\text{W/m}^2$ ) can be compared to that used for scouring membrane bioreactor (MBR) filtration membranes. Based on the analysis of Verrecht et al (2008),  $P_m$  for early-generation MBR products was approximately 10 and 5  $\text{W/m}^2$ , for flat sheet and hollow fibre membranes, respectively. This specific mixing power input was significantly reduced with the introduction of cyclic and sequential scouring, and is currently in a range of 1.0 - 2.0  $\text{W/m}^2$  (Côté et al, 2012). Therefore, the coarse bubble mixing applied to the MABR membrane is 1-2 orders of magnitude lower than for an MBR membrane. Although the MBR and MABR products look similar (Figure 2), their mixing requirements are for completely different purposes. In an MBR, large amounts of suspended solids are carried into the hollow fibre bundles and left behind by permeate removal; the role of aeration scouring is to prevent the buildup of solids within the MBR module. In an MABR, the role of mixing aeration is to renew the concentration of soluble components (e.g.; organic carbon and ammonia) at the biofilm surface, not to remove suspended solids and therefore a lower aeration intensity can be expected.

### **aeration efficiency**

A key benefit of an MABR is to reduce the energy needed for aeration. Typically, bubble diffusion can transfer 1 to 2 kg  $\text{O}_2/\text{kWh}$  (Rosso et al, 2005). Values of 3 to 4, and up to 5 kg  $\text{O}_2/\text{kWh}$  were obtained in this study, but the technology can deliver more. Figure 11 was prepared using Equation 4 to illustrate the relationship between oxygen flux (J) and aeration efficiency (AE) for the conditions used in this study (solid red curve) and optimized conditions. The red line describes the experimental results well as an AE of 4 kg  $\text{O}_2 / \text{kWh}$  corresponds to an oxygen flux of 15 g/d/m<sup>2</sup> (red dot) as can be seen in Figure 6.

Optimized conditions represented by the red dashed line result from reducing the process air flow rate (as demonstrated during days 71-90) and reducing the pressure loss through the hollow fibers by using a slightly larger inside diameter; the combined effect of these two changes would reduce the process feed pressure from 67 to 40 kPa. This analysis shows that it is possible to optimize the process to maintain an aeration efficiency greater than 6 kg  $\text{O}_2 / \text{kWh}$ , a factor of about 4 better than conventional bubble aeration.

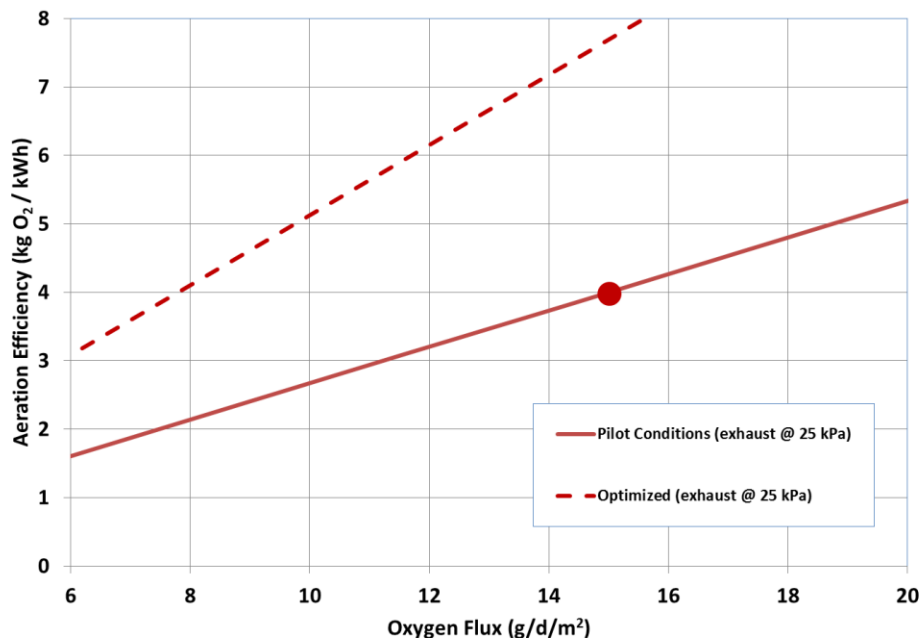


**Figure 11. Process conditions and aeration efficiency**

## conclusions

It was demonstrated that the hybrid MABR process can remove nitrogen via the conventional nitrification/denitrification pathway in a low/no dissolved oxygen environment.

Nitrification rate varied with ammonia loading rate and was 1.5 to 3.0 g  $\text{NH}_4\text{-N/d/m}^2$  for the three reactors in aggregate, achieving an effluent ammonia concentration of <5.0 mg/L. Nitrification rates were not reduced by the presence of readily biodegradable COD when compared to a similar data set obtained with a synthetic ammonia solution. COD removal occurred primarily through denitrification in the anoxic suspended biomass. Significant denitrification was achieved without nitrate recycling.

The new MABR membrane product can operate in a high MLSS environment, making it suitable for use in a conventional activated sludge reactor to increase oxygen transfer and nitrification capacity.

It was demonstrated that the new aeration membrane transfers oxygen efficiently, with a measured aeration efficiency of 3 to 5 kg  $\text{O}_2/\text{kWh}$  and the potential to reach 6 kg  $\text{O}_2/\text{kWh}$ . This step-change in energy consumption for biological treatment and nitrogen removal can significantly reduce the energy consumption for municipal sewage treatment and contribute to energy neutral wastewater treatment.

## references

- Adams, N., Hong, Y., Ireland, J., Koops, G.H. and Côté, P. (2014) A New Membrane-Aerated Biofilm Reactor (MABR) for Low Energy Treatment of Municipal Sewage. *Singapore International Water Week, (SIWW), Singapore*
- Côté, P., Alam, Z., and Penny, J., (2012) Hollow Fiber Membrane Life in Membrane Bioreactors (MBR). *Desalination* **288**, 145-151
- Martin, K.J. and Nerenberg, R. (2012) The membrane biofilm reactor (MBfR) for water and wastewater treatment: Principles, applications, and recent developments. *Bioresource Technology*, **122**, 83-94
- Peeters, J., Adams, N., Hong, Y. , Koops, G.H. and Côté, P. (2015) A New Membrane-Aerated Biofilm Reactor (MABR) for Wastewater Treatment. *2015 Membrane Technology Conference & Exposition*, Orlando, FL
- Peeters, J., Vicevic, G. Koops, G.H. and Cote, P. (2014a) The Role of Innovative Technologies in Achieving Energy-Neutral Wastewater Treatment. *Singapore International Water Week, (SIWW), Singapore*
- Peeters, J., Vicevic, G., Syed, W. and Côté, P. (2014b) MBR with Enhanced Primary Treatment to Reduce Energy Consumption. *Singapore International Water Week, (SIWW), Singapore*
- Rosso, D., Iranpour, R. and Stenstrom, M.K. (2015) Fifteen Years of Offgas Transfer Efficiency Measurements on Fine-Pore Aerators: Key Role of Sludge Age and Normalized Air Flux. *Water Environ. Res.*, **77** (3), 266-273
- Stewart, P.S. (2003) Diffusion in Biofilms. *Journal of Bacteriology*, **185** (5), 1485-1491
- Syron, E. and Casey, E. (2008) Membrane-Aerated Biofilms for High Rate Bio-treatment: Performance Appraisal, Engineering Principles, Scale-up, and Development Requirements. *Environmental Science and Technology*, **42** (6), 1833-1844
- Verrecht, B., Judd, S., Guglielmi, G., Brepols, C. and Mulder, J.W. (2008) An Aeration Energy Model of an Immersed Membrane Bioreactor. *Water Research*, **42**, 4761-4770
- Water Environment Federation (WEF) (2011) Biofilm Reactors, *WEF Manual of Practice No. 35*